Kochi Chapter

Indian Geotechnical Conference
IGC 2022
15th – 17th December, 2022, Kochi

Micromechanical insights on the stiffness of sands through grain-scale tests and DEM analyses

Nallala S.C Reddy[1], Kostas Senetakis[2] and Huan He[3]
[1]PhD student, Department of Architecture and Civil Engineering, City University of Hong Kong, China
[2]Associate Professor, Department of Architecture and Civil Engineering, City University of Hong Kong, China
[3] Associate Professor, Institute of Geotechnical Engineering, Southeast University, Nanjing, China
corresponding author e-mail: *scnallala-2@my.cityu.edu.hk*

ABSTRACT

The study of granular material behavior at multi-scales, i.e., macro, meso, and microscale through discrete element method (DEM) simulations calibrated with the macroscopic experimental data is the most common approach. However, this approach involves arbitrarily choosing the important particle contact parameters (density, contact normal and tangential stiffness, contact friction) used as input in DEM simulations which greatly affect the fabric formation and thereby influence the stress-strain response of granular materials. Therefore, a new micromechanical- based contact modeling approach is proposed in the present study where the particle contact properties are derived from micromechanical (grain-scale) tests (a range is suggested for normal contact stiffness and contact friction values) and are used as a reference for developing the DEM model. The DEM model analysis was implemented using a micromechanical-based contact modeling approach to assess the small-strain shear modulus (G_{max}) behavior of sands. Multiscale insights were drawn while evaluating the influence of contact parameters such as particle Young's modulus (E) and interparticle friction (μ) on the G_{max} behavior of quartz sand. Additionally, the real sand grain contact characteristics evaluated using micromechanical tests along with the DEM analysis provided new insights into the roughness characteristics of granular materials.

Keywords: *Contact stiffness; DEM; micro-mechanical based contact modeling; contact parameters, surface roughness*

1. Introduction

The mechanical behavior of granular materials is mainly attributed to the grain interaction happening at the contact interfaces owing to their varied morphological features (Sandeep and Senetakis, 2018, 2019). Thus, assessing their behavior involves conducting multi-scale analysis (through experimental and numerical investigations) and implementing micromechanical-based concepts to obtain insights into the complex micro mechanisms which influence their macroscale response. Specifically, the development of the discrete element-based modeling (DEM) approaches has allowed researchers to gain new insights into the micromechanical behavior of geological and artificial materials. Furthermore, DEM analysis also helps in understanding the constraints that influence the macroscale behavior during element-size tests such as boundary influence, size effect, and gradation (O'Sullivan., 2011; Huang et al., 2014). This has motivated researchers to use DEM to analyze geotechnical problems such as landslides, avalanches, and debris flow where discrete particle interaction places an important role in deciding the mechanical response of the granular system.

Using DEM analysis for assessing the complex phenomenon/mechanisms involves choosing some important input parameters which define the grain contact behavior, for example, normal and tangential load-displacement relationship, friction behavior, and grain crushing strength. Apparently, these parameters cannot be obtained from assessing the macroscale experimental data. It was only recently possible to obtain this data through the use of high precision grain-scale testing apparatus that allows the quantification of grain contact properties such as contact stiffness (normal and tangential) and friction in the study of grain-grain type contacts (Cole et al., 2007; Senetakis and Coop, 2014). This new information gives a fundamental understanding of the grain contact mechanism and

helps to validate the contact models used in DEM analysis along with providing information on the contact input parameters. This is particularly important for the modeling of different variants of soils and evaluating their multiscale behavior.

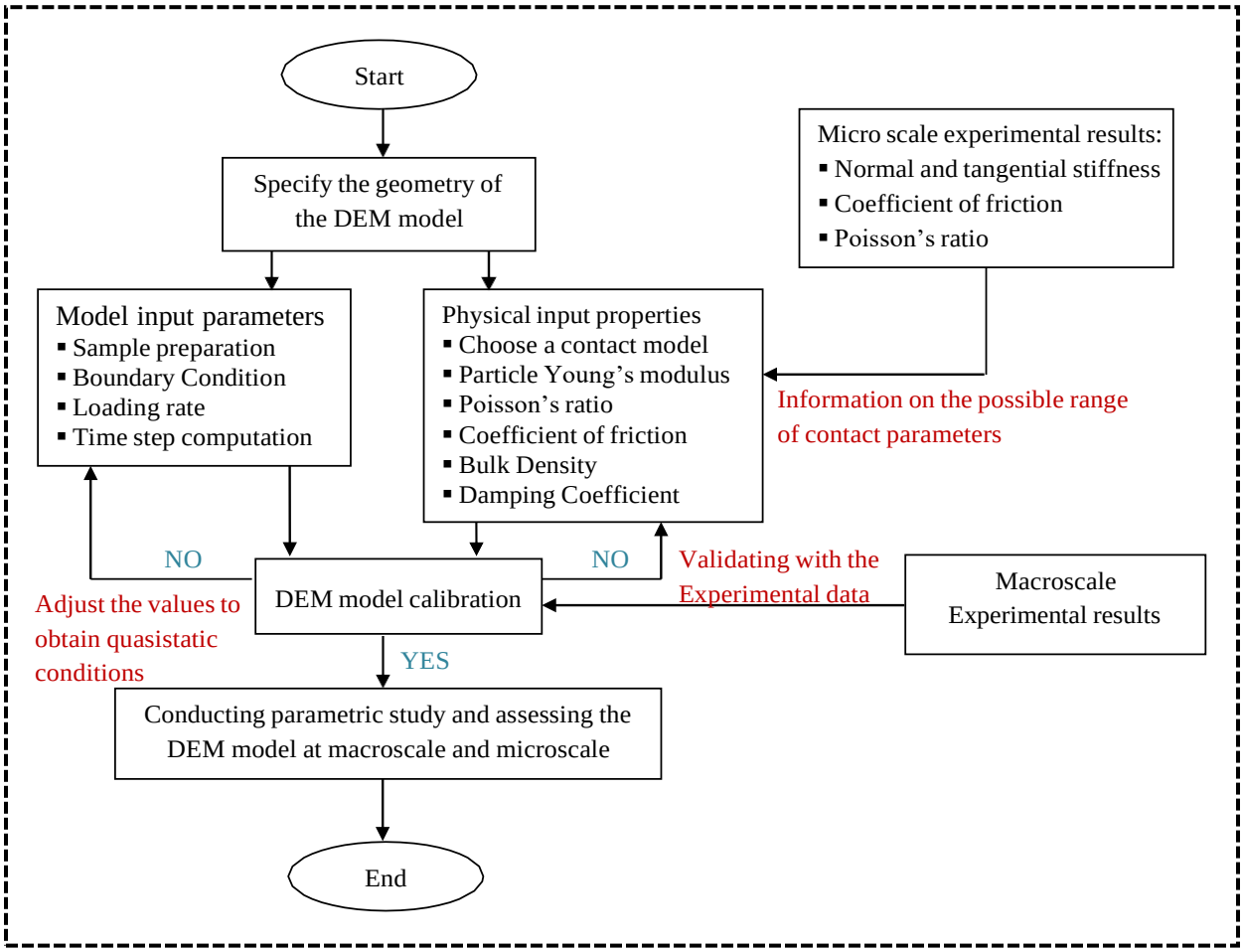

Figure 1 Flow chart illustrating the proposed approach

This article provides a brief summary of the paper by Reddy et al., 2022 along with some new insights through additional experimental and numerical analysis. The Flow chart shown in Figure 1 demonstrates the proposed micromechanical contact modelling based discrete element approach. Firstly, the standard micromechanical tests were conducted on a few sets of sand grains to obtain contact stiffness and friction data which are crucial inputs for numerical modeling. Secondly, the contact input parameters for calibrating the discrete element model were selected from the parameters range suggested from the given set of grain-scale tests on sand grains. Consecutively, a parametric study was conducted with macroscale and microscale observations discussed using necessary indicators/parameters. The above approach involving both experimental and numerical works was demonstrated by assessing the small-strain shear modulus (G_{max}) behavior of dry cohesionless sands.

2. Micromechanical testing of sand particles

2.1 Experimental apparatus and procedure

The interparticle testing apparatus used to conduct grain scale tests was developed at the City University of Hong Kong (Senetakis and Coop, 2014). This apparatus can be used to conduct tests in the order of microscale to assess the normal and tangential force-displacement response of the sand size grains ranging from 0.8-5 mm. Figure 2 shows the picture of the interparticle apparatus along with a flow chart explaining the experimental procedure for the micromechanical test and a schematic showing the grain arrangement during the application of normal and tangential loading. The main components of the current version of the apparatus (shown in Figure 2) include a stiff loading frame, a sled both of which are made of stainless steel, and three loading arms i.e., two in the horizontal direction and one in the vertical direction. Each of these loading arms constitutes a linear stepper motor and load cells (connected using stiffer connections) to apply the required quantity of load in the given direction. Each of the above-mentioned systems constitute a load cell of 100 N capacity with a resolution of 0.02 N, and a displacement sensor of non-contact type with ±3 mm measurement range and 0.01 μm of resolution. A detailed description of the apparatus and studies on a broad range of grain interfaces has been presented and discussed in previous literature (e.g., Senetakis and Coop 2014; Nardelli and Coop., 2016; Sandeep et al., 2018, 2019; Kasyap and Senetakis, 2019). In the present study, the interparticle apparatus was used to conduct standard micromechanical tests on Leighton Buzzard sand (LBS) (a variant of quartz sand) of diameter in the range of 1.18-2.36 mm, and the stiffness and friction data were used as reference later in the development of DEM model and study the small-strain behavior of sands.

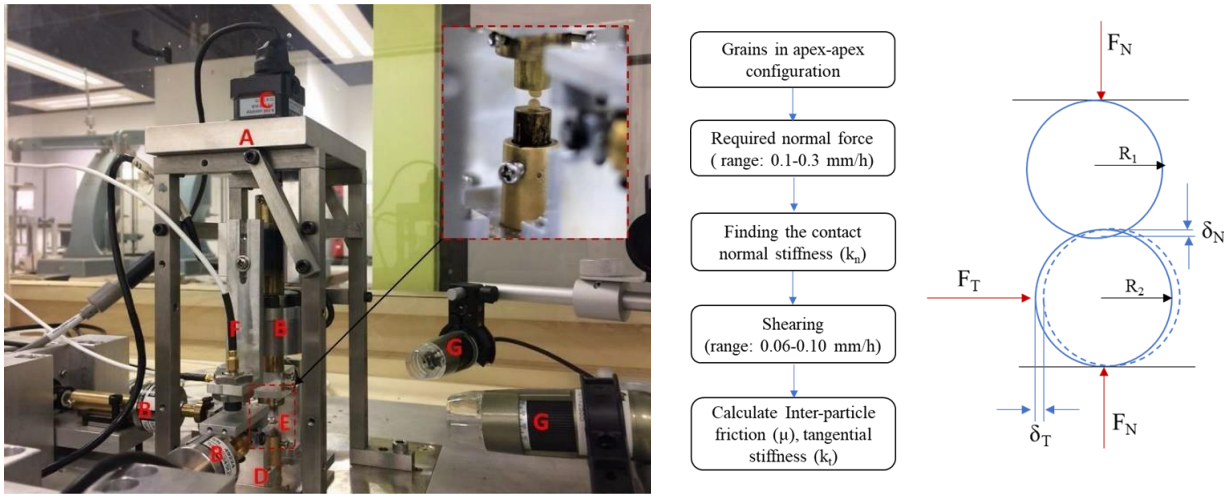

Figure 2 Inter-particle testing apparatus consists of a) Stiff loading frame b) load cell c) linear actuator d) sled placed on chrome steel balls e) soil particles during test f) eddy-current displacement sensor g) Digital micro cameras (after Sandeep and Senetakis, 2018b)

2.2 Normal contact behavior

The normal force-displacement curves for the tested sets of LBS-type sand grains are shown in Figure 3(a) along with the reference curves from literature for sand-type grains (Nardelli and Coop., 2016; Sandeep et al., 2018). It can be observed from the figure that the normal force-displacement relationship is non-linear, and an initial plastic regime is observed for most of the experimental curves as shown in Figure 3(a). Similar response/behavior was

reported for different geological and reference materials in previous studies which was mainly attributed to the surface roughness properties of the selected grain. Observing the normal-force displacement curves shown in Figure 3(a), it can be noticed that there is a reasonable scatter in the curve owing to the varied morphological features for the similar grain type. Previous studies on LBS-type sand grains reveal that the theoretical range of particle Young's modulus for the normal force-displacement curves may vary from 40-110 GPa. For example, Sandeep and Senetakis., 2018 reported that the particle Young's modulus range may vary from 40-70 GPa whereas Nardelli and Coop., 2019 showed that E value can be as high as 110 GPa for LBS-type sand grains. Also, the range of contact normal stiffness (k_n) of the set of LBS grains is also presented in Figure 3(b) (Contact normal stiffness against normal displacement plot shown on the right side). From the data presented in the plot, the contact normal stiffness for LBS-type sand grains ranges from 1×10^5 N/m to 30×10^5 N/m (or even more) depending on the normal displacement (compression) of the contacting grains. This important information will help in assessing the contact characteristics of a sand particle and help in the DEM modeling of sand particles to further obtain new insights on sand particles' behavior, for example, by studying a strength or stiffness problem. Therefore, in the present study, the contact properties for the DEM model were chosen by considering the experimental findings from the grain scale tests.

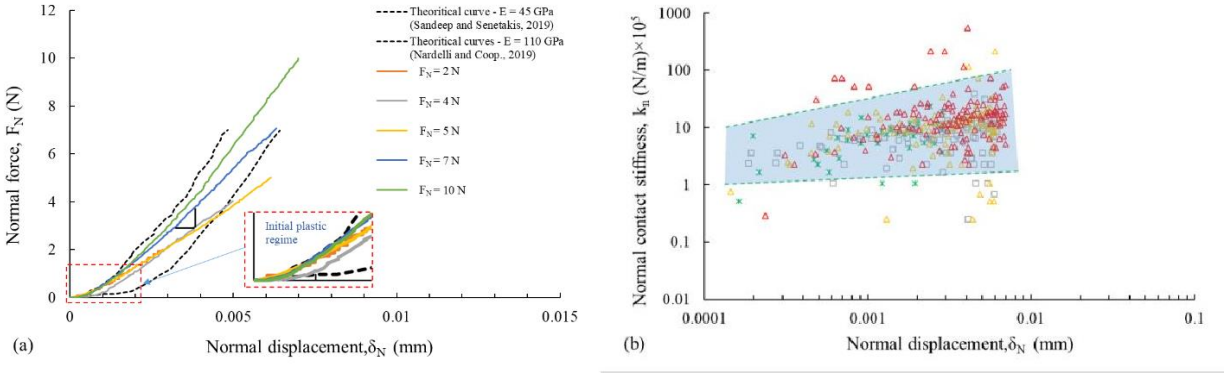

Figure 3 a) Normal force versus normal displacement curves for LBS type sand grains b) Normal contact stiffness (k_n) domain with respect to normal displacement

2.3 Tangential contact behavior

The tangential force-displacement response of sets of LBS type sand grains were captured using the horizontal force application and displacement measuring arrangement provided in the interparticle apparatus at different constant normal forces (e.g., FN = 2N, 5N, 7N, 10N). The tangential force-displacement relationship for the given set of sand grains is presented in Figure 4(a). The general trend observed for LBS type sand grains is that the tangential force increases with increase in tangential displacement until a limiting (friction mobilization) value is reached, thereafter, it almost remains constant (Sandeep et al., 2018) following Coloumb's friction criteria given by $f^{\mu}_{s,max} = \mu f_n$. The tangential force-displacement relationship (shown in Figure 4(a)) constitutes two major regimes (Sandeep and Senetakis, 2019). The first regime indicates a non-linear increase of tangential force with increase in tangential/shear displacement, while the second regime demonstrates a plastic behavior where the tangential force almost remains constant with further increase in tangential displacement. Figure 4(b) reveals that the two regimes are separated by a displacement called as the threshold displacement (also termed as slip displacement, δ_{slip}) where the tangential force changes its behavior corresponding to the displacement (Sandeep and Senetakis, 2019). Conceptually, the

threshold displacement occurs when the tangential force reaches the threshold value given as product of interparticle friction (μ) and normal force ($f^{\mu}_{s,max} = \mu f_n$). Therefore, the threshold displacement (δ_{slip}) depends on the value of the normal contact force (F_N) and friction between the grains which depend on the grain roughness and morphological features. The same is reflected in the Figure 4(b) showing the changing threshold displacement (δ_{slip}) value with change in the normal contact force (F_N). Similar behavior is expected to happen at grain scale during an element size tests on granular samples. Overall, from the shearing tests done on LBS-type sand grains, it was observed that the contact friction (μ) between the LBS grains range from 0.18-0.25 which gives an indication of its surface roughness and morphological features. In the present study, this information is used to decide the contact shearing behavior (based on Coulomb's friction criteria) of grains in the DEM analysis which is explained in the subsequent sections.

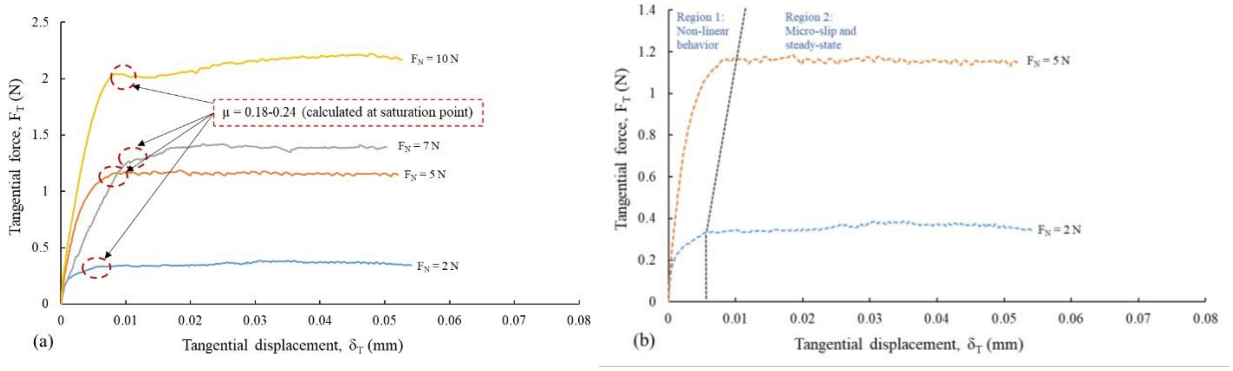

Figure 4 a) Tangential force versus tangential displacement curves for LBS type sand grains b) Plot showing the two regimes during the shearing test on LBS type sand grains

3 Discrete element analysis of sand particles

In the present study, a discrete element model was developed to simulate the consolidate drained triaxial test on quartz sand and study its small-strain shear modulus (G_{max}) behavior. The numerical model formulation employed in this study corresponds to the PFC3D program (Cundall and Stark, 1979). The spherical grains were considered to represent sand particles and the contact properties for DEM simulation were chosen based on the insights from the micromechanical tests on sand grains (as explained in the previous section). The shape-related roughness was neglected in the present study owing to the high computational cost involved in the simulation of clumps and the particle shape becomes important only when examining large strain problems or problems related to grain crushing (Jensen et al., 1999; Wu et al., 2021). However, as stress-strain response were captured at very small strains the effect of shape-related roughness becomes negligible. Importantly, the present work focuses on using real experimental micromechanical data as reference for deciding the contact parameters for the DEM analysis and investigating the influence of roughness on the normal contact stiffness and the stress-strain response.

The initial DEM sample was created using a cloud of 12983 spherical particles with the grain size distribution similar to a uniformly graded sand as shown in Figure 5. The rigid wall boundary condition was used with the servo-algorithm to obtain DEM cylindrical samples of required density/void ratio. The interparticle friction (μ) was set as 0.23 and packing pressure corresponding to the sample's final mean effective stress (p′) was used to generate the DEM samples. The contact model for simulation was the user-defined dry Hill material contact model (Potyondy, 2016) was used as it considers Hertz-Mindlin contact theory (Mindlin, 1949; Hertz 1882) to define the surface interaction between particles. In the present study, three sets of DEM samples were considered by assigning three

distinct particle Young's modulus values i.e., E = 10, 50, and 100 GPa, representing a range of sand variants. For these analyses, the μ value was set as 0.23 (which was in the range of 0.18-0.25 as observed from interparticle test results) for all the simulations. Similarly, the Poisson's ratio (υ) of 0.12 and solid density (ρ) of 2650 kg/m^3 was assigned to all the particles (Heyliger et al., 2003; Lopera Perz, 2017). Other geometrical parameters required during DEM simulation include axial strain rate and time step determination. A lower value of axial strain rate ($\dot{\varepsilon}$) in the range of 10^{-3} to 10^{-4} was set to maintain a low increment rate. The automatic timestep option (available in PFC3D) was used to calculate the time step which resulting in a time step value in the range of 10^{-7} to 10^{-8}. Therefore, the resulting incremental axial deformation (dε) was sufficiently smaller to derive the deviatoric stress (q) values at shear strains of order 10^{-5}-10^{-4} % and calculate the corresponding small-strain shear modulus (G_{max}).

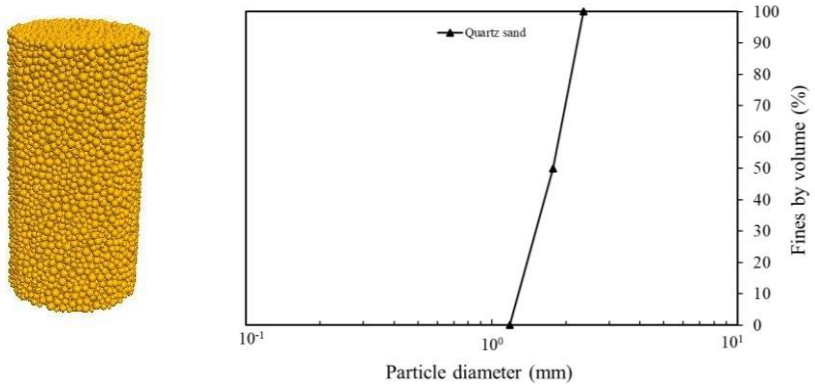

Figure 5 Grain size distribution of the numerical sample considered in the present study

Twenty numerical tests were conducted on DEM samples. The first set of tests were conducted to assess the influence of particle Young's modulus (E) on the small-strain shear modulus (G_{max}) of quartz sands. Subsequently, the effect of isotropic compression pressure (p′) on the G_{max} was also assessed and the power law fitting (based on Hardin's equation given by Hardin and Black, 1966) was used to validate the DEM model with the Experimental data of G_{max} for the quartz sands. The other set of numerical simulations was conducted to measure the effect of interparticle friction (μ = 0.2, 0.23, 0.3, 0.4, 0.6) which can indirectly represent the roughness effect (as a surface characteristic) on the G_{max} behavior of quartz sand.

3.1 Small-strain shear modulus (G_{max})

The shear modulus is a parameter generally used to represent the stiffness characteristic of geological materials. For a given material, the shear modulus can be calculated using Equation (1)

$$G = \frac{1}{3} \times \frac{dq}{d\gamma} \text{ and } \gamma = \frac{2}{3}(\varepsilon_1 - \varepsilon_2) \quad (1)$$

where dq and dγ represents the change in the deviatoric stress and shear strain, respectively. The small-strain shear modulus (G_{max}) is specifically defined at very small strains range i.e., 10^{-5}-10^{-4} % where the behavior is considered elastic (Atkinson, 2000).

Significance of particle Young's modulus (E) and its influence on G_{max}

In general, the natural sands possess varying contact properties due to varied roughness and particle Young's modulus (E) characteristics owing to the geological and morphological features of the parent rocks. For a given material type (e.g., variants of sand), contact normal stiffness (which primarily depends on E value) decreases with increase in surface roughness and vice versa. Thus, this parametric study is focused on understanding clearly the influence of particle Young's modulus (E) along with change in mean effective stress (p′) on the response of the DEM model. The DEM model response was thoroughly investigated by considering three particle Young's modulus values, i.e., E = 10 GPa, 50 GPa and 100 GPa which represent a broad range of sand variants. Additionally, the mean effective stress was also varied in the range of 50 to 300 kPa to study the coupled influence (along with parameter E) on G_{max} behavior. During the numerical simulation the other contact parameters which include possion's ratio, interparticle friction, and solid density were kept constant.

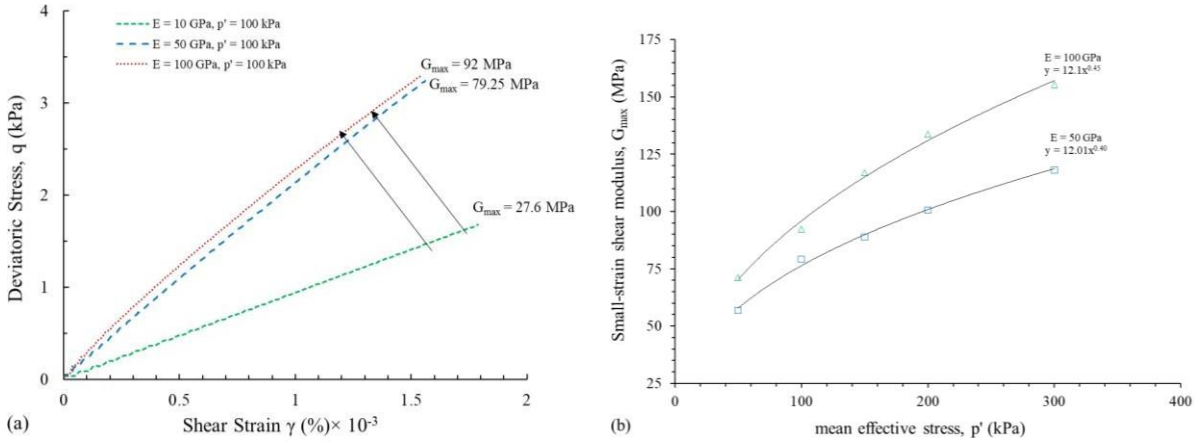

Figure 6 a) Deviatoric stress versus shear strain response for three different values of particle Young's modulus, E under a mean effective stress, p′ = 100 kPa b) G_{max} - p′ relationship based on the parametric study

Figure 6(a) presents the deviatoric stress versus shear strain curves for three representative samples with particle Young's modulus values, E = 10, 50 and 100 GPa. The slope of these curves (presented in Figure 6(a)) at shear strains less than 10^{-4}% yield the value of small-strain shear modulus (G_{max}). Figure 6(a) shows that the inclination of the curve increases predominantly as E value increases from 10 GPa to 50 GPa, however, it doesn't vary much as the E value increase further to 100 GPa. The corresponding G_{max} (calculate using Equation 1) values (shown in Figure 6(a)) also show the same trend. The convention here is that an increase in roughness leads to decrease in contact stiffness (which was simulated through decrease in particle Young's modulus), thereby resulting in lower small-strain shear modulus, G_{max} which was also observed in previous experimental studies (Senetakis et al., 2012). In Figure 6(a), the G_{max} value corresponding to the lower values of E (e.g., E = 10 GPa) may represent the highly weathered granular materials such as volcanic sands. On the other hand, the G_{max} values for the DEM samples with particle Young's modulus (E) of 50 and 100 GPa may correspond to silica-based sands with low and high roughness. Figure 6(b) shows the evolution of small-strain shear modulus with change in mean effective stress (p′) for two values of particle Young's modulus, E = 50 GPa and 100 GPa respectively. The DEM simulation results (presented in Figure 6(b)) indicate that for both values of particle Young's modulus (E), the G_{max} increases significantly with increase in mean effective stress (p′), however, the rate of increase of G_{max} with respect to mean effective stress (p′) slightly higher for samples with E = 100 GPa compared to samples with E = 50 GPa. This is demonstrated in the Figure 6(b) and power law fitting is used to assess the trend of the numerical date points. The rate of increase of G_{max} is represented by power value, i.e., 0.40 and 0.45 for samples with E = 50 and 100 GPa

respectively. The power values (i.e., n = 0.40 for E = 50 GPa and n = 0.45 for E = 100 GPa) obtained in the present numerical study are in good agreement with the experimental values for quartz sand whose general range as reported in literature is between 0.4 and 0.6 for sand type granular materials with changing grain sizes (Senetakis et al., 2012; Yang and Gu, 2013). This validates the present DEM model with respect to the macroscale experiments.

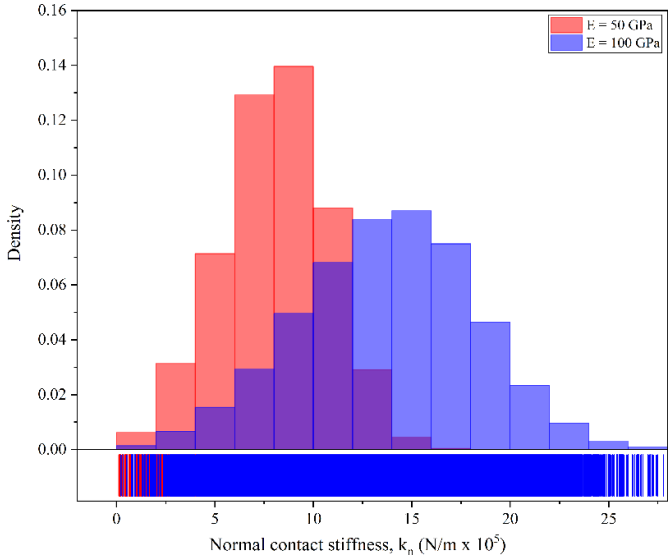

Figure 7 Bar chart showing the normal contact stiffness (k_n) of two DEM model (E = 50 GPa and 100 GPa) at G_{max} position at a mean effective stress (p′) of 100 kPa

Additionally, the Bar chart plot is presented in the Figure 7 showing the contact normal stiffness distribution among the grain contacts for samples with E = 50 and 100 GPa. These values are comparable with the contact normal stiffness values derived from the micromechanical tests on sands (referring to Figure 3). The contact model used in the DEM model simulation was able to numerically simulate the contact behavior happening at the grain scale. It can be observed that the normal contact stiffness (k_n) is distributed over a wider band as the E value increases from 50 GPa to 100 GPa. It can be presumed that the variation in distribution of normal contact stiffness (k_n) causes a change in the granular matrix formation which effects the contact force network. Therefore, the DEM model generated by varying E value may have different contact force transfer network, hence, effects the stress-strain response of the numerical sample when the triaxial test is conducted. Thus, the G_{max} which is derived from the deviatoric stress versus shear strain curve is affected by the change in particle Young's modulus.

Interparticle friction (μ) and it influence on the G_{max}

The interparticle friction (μ) is another important contact parameter which may influence the small-strain shear modulus (G_{max}) behavior. This is due to its credible contribution towards the formation of the granular matrix (Fabric). A constant value of interparticle friction (μ) of 0.23 was considered during the sample preparation and isotropic compression stage for all the DEM simulations. Thereafter, the DEM model response was captured during the triaxial test for five values of friction, i.e., μ = 0.2, 0.23, 0.3, 0.4, and 0.6 to assess the influence of interparticle friction (μ) on the G_{max} behavior of the sands. It is to be noted that slight readjustment of the grains happens (due to a change in interparticle friction, μ) before the shearing starts to maintain the corresponding mean effective stress

(p′) which affects slightly the granular fabric. The purpose of this assessment is to indirectly understand the effect of roughness (as a surface characteristic) on G_{max} behavior of sands. For this purpose, an error bar chart is presented in the Figure 8 showing the range of surface roughness for different brands of sands and their corresponding average friction values. For example, the friction value of 0.2-0.3 represents the different brands of quartz sands (where the actual value of friction is linked with the surface roughness of sand grain) (Nardelli and Coop, 2019; Sandeep et al., 2018, 2019). On the other hand, μ values of 0.3 and 0.4 may represent materials including crushed rock/stone, limestone, biogenic carbonated sands, chipped grains from weathered granite rocks (Nardelli and Coop, 2019; Ren et al., 2021b) whereas a μ values around 0.6 may represent materials such as grains from pumice rock origin (He and Senetakis, 2019). General trend is that the interparticle friction (μ) increases with increase in surface roughness, however, for certain variants of sands this correlation may not be true. For example, the average value of friction for CDG grain (μ_{avg} = 0.37) is lower than tailing sand (μ_{avg} = 0.41) though the surface roughness of CDG grains is relatively higher than Tailing sand. This behavior may be linked to the stiffness characteristics of the respective grains.

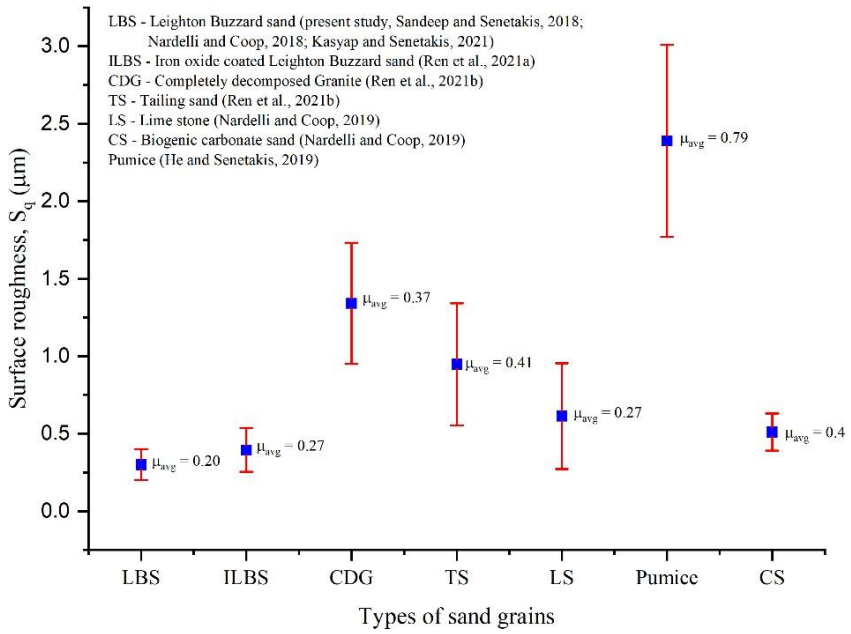

Figure 8 Surface roughness ranges of different brands of sand and their corresponding average friction

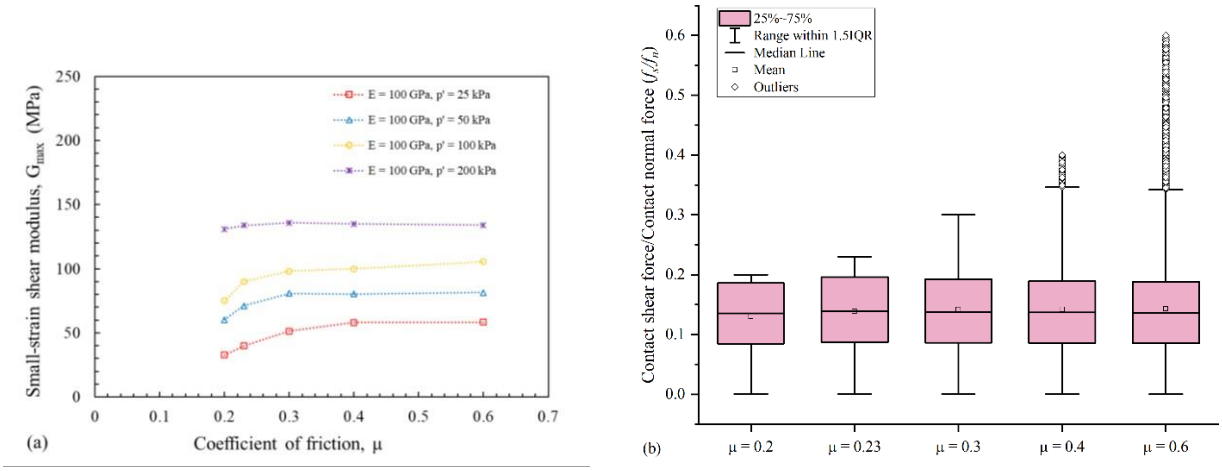

Figure 9 a) G_{max} variation with interparticle friction at different mean effective streses (p′) b) Box plots showing the contact shear force contribution with respect to contact normal force (at G_{max} position) for different values of interparticle friction (μ) considering E = 100 GPa and p′ = 50 kPa

The contact model used in the present study considers Columb's friction criteria ($f^{\mu}_{s,max} = \mu f_n$) to control tangential force contribution thereby the particle movement (slippage) which causes chage of fabric during the triaxial test. Therefore, the influence of interparticle friction (μ) on the G_{max} is investigated. Figure 9(a) shows the variation of G_{max} with an increase in interparticle friction (μ) for a representative DEM sample (E = 100 GPa). This G_{max} trend was captured at four different values of mean effective stresses (p') i.e., p′ = 25, 50, 100, and 200 kPa. From the figure, it can be noticed that the G_{max} is significantly affected by change in the mean effective stress (p′) owing to the increase in the denseness of the sample. It can be observed that G_{max} tends to increase noticeably at lower values of interparticle friction, μ = 0.2 to 0.4 given the mean effective stress acting on the sample is lower (e.g., p′ = 25 and 50 kPa). This trend changes as p′ increases from 25 to 200 kPa, thereby decreasing the influence of interparticle friction (μ) on G_{max}. On the other hand, at all values of mean effective stress, the influence of friction (μ) on G_{max} is negligible for values of μ > 0.4. Therefore, it can be stated that the role of roughness in controlling G_{max} is majorly contributed through the contact normal stiffness (k_n) (which indirectly depends on the Young's modulus) and may not be due to interparticle friction (μ), for material with relatively high roughness (i.e., resulting in a higher value of μ). This can be further verified by observing Figure 9(b), where the ratio of shear force and normal force (f_s/f_n) is presented (through a box chart) using the contact data captured at G_{max} position for samples with different values of interparticle friction, μ = 0.2, 0.23, 0.3, 0.4, and 0.6. Figure 9(b) shows that the quartile (25% to 75%) range of values of the ratio (f_s/f_n) only varied slightly as the interparticle friction (μ) varied from 0.2 to 0.3, thereafter, the variation in almost negligible. Therefore, as the quartile represents the behavior of large number of particles in the DEM sample, the DEM response (i.e., G_{max} in the present study) is not significantly affected by the interparticle friction (μ) specifically at higher values of μ.

5. Conclusions

The stiffness properties of a uniform packing of spheres which represent quartz sand were investigated through grain scale tests at the microscale and numerically evaluated at the macroscale using DEM simulations. The grain scale tests were conducted on sand particles and the normal and tangential force-displacement responses of the representative set of sand grains were captured giving information on the general range of contact normal stiffness (k_n) and coefficient of interparticle friction (μ) for sand grains. Additionally, the grain-scale tests also demonstrate

the changing tangential contact behavior with increase in load and displacement through the concept of micro-slip displacement which explains the grain interaction that may happen during shearing during an element size test on sands. The Discrete element models were developed by choosing contact properties based on the assessment of the realistic particle properties (which is given as a range) of sand obtained from grain-scale tests. The Discrete element model so developed was validated with the data obtained from element size (macroscale) test indirectly by matching the power law fitting values (n) of the G_{max} of the DEM samples with the common range of n values for sand variants from the literature. The G_{max} behavior of different brands of sands (sands with low to high contact normal stiffness) was assessed by considering particle Young's modulus values over a broader range (e.g., E = 10, 50 and 100 GPa) keeping other parameters constant. The numerical results showed that an increase in E value caused an increase in G_{max} which implies a direct influence of contact normal stiffness distribution on the stress-strain response. Additionally, this also affected the shear modulus and mean effective stress relationship which was assessed using power law fitting of the numerical data of G_{max}. These results provided a new prospective on the influence of roughness of granular materials (introduced through particle Young's modulus) whose increase decreases the macroscopic stiffness (G_{max}) due to its influence on contact normal stiffness. These observations provide a numerical justification for the reduced macroscopic stiffness for granular mixtures such as sand-silt mixtures and sand-clay mixtures which was also suggested by previous experiments.

For a given DEM sample with constant initial fabric obtained by keeping contact interparticle friction during the sample preparation stage, the increase in interparticle friction from 0.2 to 0.4 during the DEM triaxial loading caused an increase in G_{max}. On the other hand, at larger values of $\mu > 0.4$, the G_{max} was independent of interparticle friction (μ). Specifically, the influence of interparticle friction (μ) on G_{max} was predominant at a lower range of mean effective stress values ($p' < 100$ kPa) than at higher values ($p' > 100$ kPa). The observed G_{max} behavior is linked with the increase in stability of contact force chains which are directly related to the shear force contribution which is controlled using the Coulomb's friction criteria. Overall, qualitative analysis of the observed G_{max} trend showed that it was predominantly influenced by normal contact stiffness (which affects the normal force contribution) rather than due to interparticle friction which controls the shear force contribution in the DEM model simulations.

Acknowledgements

The work described in this paper was fully supported by a grant from the Research Grants Council of the Hong Kong Special Administrative Region, China, Project No. "CityU 11210419" and a DON fund, Project No. "9220117".

References

Atkinson, J. H. (2000). Non-linear soil stiffness in routine design. *Géotechnique, 50*(5), 487-508. doi:10.1680/geot.2000.50.5.487.

Cundall, P.A., & Strack, O.D.L. (1979). A discrete numerical model for granular assemblies. *Geotechnique 29 (1)*, 47–65.

Cole, D. M., & Peters, J. F. (2007). Grain-scale mechanics of geologic materials and lunar simulants under normal loading. *Granular Matter, 10*(3), 171-185. doi:10.1007/s10035-007-0066-y.

Hardin, B. O., & Black, W. L. (1966). Sand Stiffness Under Various Triaxial Stresses. *Journal of the Soil Mechanics and Foundations Division, 92*(2), 27-42, doi:10.1061/JSFEAQ.0000865.

Heyliger, P., Ledbetter, H., & Kim, S. (2003). Elastic constants of natural quartz. *J Acoust Soc Am, 114*(2), 644-650. doi:10.1121/1.1593063.

Huang, X., Hanley, K. J., O'Sullivan, C., Kwok, C. Y., & Wadee, M. A. (2014). DEM analysis of the influence of the intermediate stress ratio on the critical-state behaviour of granular materials. *Granular Matter, 16*(5), 641-655. doi:10.1007/s10035-014-0520-6.

He, H., Senetakis, K. (2019). An experimental study on the micromechanical behavior of pumice. *Acta Geotechnica*, 14(6), 1883-1904.

Jensen, R. P., Bosscher, P. J., Plesha, M. E., & Edil, T. B. (1999). DEM simulation of granular media-structure interface: effects of surface roughness and particle shape. *Int. J. Numer. Anal. Meth. Geomech, 23*(6), 531-547. doi:10.1002/(SICI)1096-9853(199905)23:6<531::AID-NAG980>3.0.CO2-V.

Kasyap, S. S., & Senetakis, K. (2019). Interface load–displacement behaviour of sand grains coated with clayey powder: Experimental and analytical studies. *Soils and Foundations, 59*(6), 1695-1710. doi:https://doi.org/10.1016/j.sandf.2019.07.010.

Lopera Perez, J. C., Kwok, C. Y., & Senetakis, K. (2017). Investigation of the micro-mechanics of sand–rubber mixtures at very small strains. *Geosynthetics International, 24*(1), 30-44. doi:10.1680/jgein.16.00013.

Mindlin, R. D. (1949). Compliance of Elastic Bodies in Contact. *Journal of Applied Mechanics, 16*, 259–268.

Nardelli, V., & Coop, M. R. (2016). The Micromechanical Behaviour of a Biogenic Carbonate Sand. *Procedia Engineering, 158*, 39-44. doi:10.1016/j.proeng.2016.08.402.

Nardelli, V., & Coop, M. R. (2019). The experimental contact behaviour of natural sands: normal and tangential loading. *Géotechnique, 69*(8), 672-686. doi:10.1680/jgeot.17.P.167.

O'Sullivan, C. (2011). Particle-Based Discrete Element Modeling: Geomechanics Perspective. *International Journal of Geomechanics, 11*(6), 449-464. doi:10.1061/(asce)gm.1943-5622.0000024

Potyondy, D. (2016). *Hill Contact Model [version 4]*. Itasca Consulting Group, Inc., Technical Memorandum ICG7795-L, Minneapolis, Minnesota.

Sandeep, C. S., & Senetakis, K. (2018). Grain-scale mechanics of quartz sand under normal and tangential loading. *Tribology International, 117*, 261-271. doi:10.1016/j.triboint.2017.09.014.

Sandeep, C. S., & Senetakis, K. (2019). An experimental investigation of the microslip displacement of geological materials. *Computers and Geotechnics, 107*, 55-67. doi:https://doi.org/10.1016/j.compgeo.2018.11.013.

Sandeep, C. S., Li, S., & Senetakis, K. (2021). Scale and surface morphology effects on the micromechanical contact behavior of granular materials. *Tribology International, 159*. doi:10.1016/j.triboint.2021.106929.

Senetakis, K., Anastasiadis, A., & Pitilakis, K. (2012). The Small-Strain Shear Modulus and Damping Ratio of Quartz and Volcanic Sands. *Geotechnical Testing Journal, 35*(6). doi:10.1520/gtj20120073

Senetakis K., C. M. R. (2014). The development of a new micro-mechanical inter-particle loading apparatus. *Geotechnical Testing Journal, 37*(6), 1028-1039.

Reddy, N. S. C., He, H., & Senetakis, K. (2022). DEM analysis of small and small-to-medium strain shear modulus of sands. *Computers and Geotechnics, 141*, doi:10.1016/j.compgeo.2021.104518.

Ren, J., Li, S., He, H., & Senetakis, K. (2021a). The tribological behavior of iron tailing sand grain contacts in dry, water and biopolymer immersed states. *Granular Matter*, 23(1), 1-23.

Ren, J., He, H., Lau, K.-C., & Senetakis, K. (2021b). Influence of iron oxide coating on the tribological behavior of sand grain contacts. *Acta Geotechnica, 17*(7), 2907-2929. doi:10.1007/s11440-021-01367-7.

Wu, M., Xiong, L., & Wang, J. (2021). DEM study on effect of particle roundness on biaxial shearing of sand. *Underground Space, 6*(6), 678-694. doi:10.1016/j.undsp.2021.03.006.

Yang, J., & Gu, X. Q. (2013). Shear stiffness of granular material at small strains: does it depend on grain size? *Géotechnique, 63*(2), 165-179. doi:10.1680/geot.11.P.083